JCI The Journal of Clinical Investigation

Coagulation factor V^{A2440G} causes east Texas bleeding disorder via TFPIα

Lisa M. Vincent, … , Dianna M. Milewicz, Björn Dahlbäck

J Clin Invest. 2013;123(9):3777-3787. https://doi.org/10.1172/JCI69091.

Research Article

The autosomal dominantly inherited east Texas bleeding disorder is linked to an *A2440G* variant in exon 13 of the *F5* gene. Affected individuals have normal levels of coagulation factor V (FV) activity, but demonstrate inhibition of global coagulation tests. We demonstrated that the *A2440G* mutation causes upregulation of an alternatively spliced *F5* transcript that results in an in-frame deletion of 702 amino acids of the large activation fragment, the B domain. The approximately 250-kDa FV isoform (FV-short), which can be fully activated by thrombin, is present in all *A2440G* carriers' plasma (n = 16). FV-short inhibits coagulation through an indirect mechanism by forming a complex with tissue factor pathway inhibitor-α (TFPIα), resulting in an approximately 10-fold increase in plasma TFPIα, suggesting that the TFPIα:FV-short complexes are retained in circulation. The TFPIα:FV-short complexes efficiently inhibit thrombin generation of both intrinsic and extrinsic coagulation pathways. These data demonstrate that the east Texas bleeding disorder–associated $F5^{A2440G}$ leads to the formation of the TFPIα:FV-short complex, which inhibits activation and propagation of coagulation.

Coagulation factor V^{A2440G} causes east Texas bleeding disorder via TFPIα

Lisa M. Vincent,[1] Sinh Tran,[2] Ruzica Livaja,[2] Tracy A. Bensend,[1] Dianna M. Milewicz,[1] and Björn Dahlbäck[2]

[1]Department of Internal Medicine, Division of Medical Genetics, University of Texas Health Science Center at Houston, Houston, Texas, USA.
[2]Department of Laboratory Medicine, Clinical Chemistry, Lund University, University Hospital, Malmö, Sweden.

The autosomal dominantly inherited east Texas bleeding disorder is linked to an *A2440G* variant in exon 13 of the *F5* gene. Affected individuals have normal levels of coagulation factor V (FV) activity, but demonstrate inhibition of global coagulation tests. We demonstrated that the *A2440G* mutation causes upregulation of an alternatively spliced *F5* transcript that results in an in-frame deletion of 702 amino acids of the large activation fragment, the B domain. The approximately 250-kDa FV isoform (FV-short), which can be fully activated by thrombin, is present in all *A2440G* carriers' plasma ($n = 16$). FV-short inhibits coagulation through an indirect mechanism by forming a complex with tissue factor pathway inhibitor-α (TFPIα), resulting in an approximately 10-fold increase in plasma TFPIα, suggesting that the TFPIα:FV-short complexes are retained in circulation. The TFPIα:FV-short complexes efficiently inhibit thrombin generation of both intrinsic and extrinsic coagulation pathways. These data demonstrate that the east Texas bleeding disorder–associated $F5^{A2440G}$ leads to the formation of the TFPIα:FV-short complex, which inhibits activation and propagation of coagulation.

Introduction

Coagulation factor V (FV) is a cofactor protein that can both promote and inhibit coagulation (1, 2). Located on 1q24–25, the *F5* gene is composed of 25 exons that transcribe a 6.8-kb mRNA (3–7). The translated 330- kDa glycoprotein precursor contains 2,196 amino acids organized into the domain structure A1-A2-B-A3-C1-C2 and is highly homologous to factor VIII (FVIII), sharing 35%–40% identity in the A and C domains (4, 5, 8). Human FV is primarily produced by hepatocytes and circulates in plasma as an intact 330-kDa precursor at a concentration of about 20 nM (7 μg/ml) (9–12). Approximately 20% of the total human FV found in whole blood is stored in platelet α granules in a partially proteolyzed form in conjunction with the binding protein multimerin. This platelet FV derives from the plasma FV pool and is secreted upon platelet activation to create a high, localized concentration of the cofactor at sites of injury (12–15).

The procoagulant cofactor function of FV is primarily dictated by its interaction and cleavage by thrombin and active factor X (FXa). Its cleavage by thrombin is deemed the most biologically important early event in the blood clot formation process (16–19). As an intact single-chain precursor, FV expresses less than 1% of its potential procoagulant cofactor activity (20). Upon sequential cleavage of Arg-709, Arg-1018, and Arg-1545 by thrombin, the large connecting B domain is removed from the intact FV molecule to produce the heavy chain (A1-A2) and the light chain (A3-C1-C2) that have M_rs of 105,000 and 74,000, respectively. The heavy chain and the light chain noncovalently associate in the presence of calcium to produce an active procoagulant cofactor (FVa). FVa and FXa assemble on negatively charged phospholipid (PL) membranes to form the prothrombinase (PTase) complex. The presence of FVa in this complex greatly accelerates the activation of prothrombin to α-thrombin by 300,000-fold relative to the activation by FXa alone (20). This activity is downregulated through activated protein C–mediated (APC-mediated) cleavages at Arg-506, Arg-306, and Arg-679 in FV. Cleavage at Arg-306, which occurs 20-fold more rapidly in the presence of protein S, completely inhibits FVa cofactor function (1, 21–23).

Recently, FV in plasma was demonstrated to interact with tissue factor pathway inhibitor-α (TFPIα), and this interaction affects TFPIα plasma concentrations, with TFPIα levels being approximately 70% lower in plasma from FV-deficient patients relative to normal plasma (24). Moreover, immunodepletion of FV in normal plasma decreased TFPIα levels by approximately 60%–90%. Surface plasmon resonance analysis using immobilized TFPIα demonstrated half-maximum binding at 13.5 nM FV. TFPI is a multivalent Kunitz-type protease inhibitor that regulates tissue factor–induced (TF-induced) coagulation by inhibiting FXa and FVIIa (25) and exists in multiple alternatively spliced isoforms. The full-length isoform TFPIα is a 276-residues long glycoprotein (approximately 40 kDa) that contains 3 tandem Kunitz-type domains followed by a basic C terminus. In plasma, the total TFPI concentration is approximately 70 ng/ml (1.6 nM), with TFPIα only constituting approximately 20% of the total TFPI in plasma. TFPIα is also present on the surface of endothelium, where it is partly bound to proteoglycans. A truncated TFPI, which lacks the third Kunitz domain and the C-terminal peptide, is the major isoform of TFPI in plasma (approximately 80%). It circulates bound to the lipoproteins, mainly to LDL (25). Another truncated isoform denoted TFPIβ is present on endothelium, where it is bound with a GPI anchor (26). Recently, Ndonwi et al. demonstrated that the positively charged C terminus of TFPIα contains the binding site for FV (27). The characteristics of the binding site in FV remain to be elucidated, but it is noteworthy that both FV and FVa were shown to bind TFPIα.

In 2001, a novel moderately severe autosomal dominant bleeding disorder was described in a large family from east Texas (OMIM 605913; family pedigree in ref. 28 and Supple-

Authorship note: Lisa M. Vincent and Sinh Tran contributed equally to this work. Dianna M. Milewicz and Björn Dahlbäck are co–senior authors.

Conflict of interest: The authors have declared that no conflict of interest exists.

Citation for this article: *J Clin Invest.* 2013;123(9):3777–3787. doi:10.1172/JCI69091.

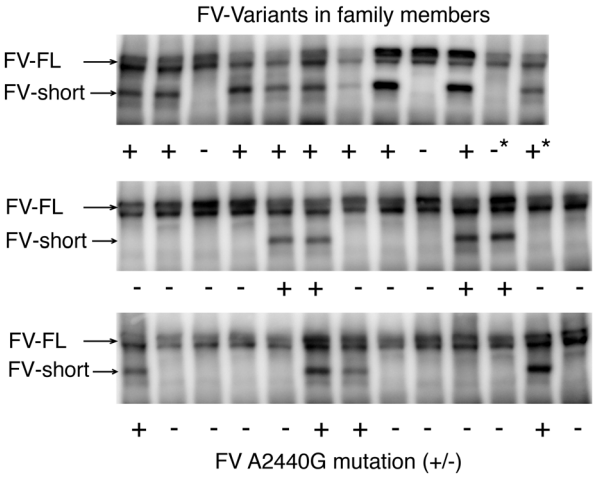

Figure 1
Immunoblot analysis of factor V derived from plasma of family members. Western blot analysis of plasma (equivalent to 0.5 μl) from affected and unaffected family members with FV being detected using the monoclonal AHV-5146 against the heavy chain in combination with HRP-conjugated goat anti-mouse antiserum. Blots were developed with Supersignal West Dura Extended Duration Chemiluminescence Substrate. The SDS-PAGE (4%–15%) was run under nonreducing conditions. Lanes marked with plus signs represent affected individuals carrying the A2440G mutation, whereas those marked with minus signs represent unaffected family members. The arrows point at full-length FV (FV-FL) and FV-short. The 2 lanes in the upper row that are marked with asterisks represent pools of unaffected (–*) and affected (+*) family members. Note the weak FV-short band in the seventh sample from the left in the upper row, the sample being derived from individual IV:17 in family pedigree (Supplemental Figure 1).

mental Figure 1; supplemental material available online with this article; doi:10.1172/JCI69091DS1). Affected family members have prolonged prothrombin time (PT) and/or activated partial thromboplastin time (APTT) even though they have normal concentrations of the coagulation factors. The disease was linked to the *F5* gene and an A→G mutation at position 2440 in exon 13, predicting replacement of serine 756 in the B domain with a glycine segregated with disease in the family with LOD score of 7.22. This position is highly conserved at both the nucleotide and protein levels among all primates and most placental mammals (Supplemental Figure 2; http://genome.ucsc.edu/, and ref. 29). In addition, no missense variants within this codon have been observed in either the 1000 Genomes Project (www.1000genomes.org) or the NHLBI Grand Opportunity Exome Sequencing Project (https://esp.gs.washington.edu/drupal/). It was originally presumed that A2440G was not a disease-causing mutation because FV clotting assays were normal and the variant is in exon 13, which encodes the large B domain that is not part of active FVa (1, 2, 30). We have now elucidated the complicated and indirect mechanisms through which A2440G produces the bleeding disorder. The A2440G mutation causes a splicing event in exon 13 that creates an in-frame removal of 2,106 base pairs that predicts a loss of 702 amino acids from the B domain. The resulting approximately 250-kDa truncated FV, termed FV-short, forms a complex with TFPIα and increases its plasma concentration dramatically. The high concentration of TFPIα:FV-short complexes in affected family members efficiently inhibits coagulation, thus causing the bleeding phenotype seen in this disorder.

Results

Short form of factor V identified in affected family members' plasma. Plasma from individual family members was analyzed by immunoblotting using a specific antibody against the heavy chain of FV (AHV-5146) to determine whether the genomic FV variant A2440G in affected patients had any observable effect on protein production or size (Figure 1). Full-length FV (FV-FL) was observed as a heterogeneous doublet band in both affected and unaffected individuals. In the plasma of all affected individuals, there was a clearly visible, unique band at ~250 kDa, termed FV-short, that was not detected in unaffected family members. Analysis of plasma samples from available family members (n = 36) demonstrated that FV-short was only found in individuals with the A2440G variant (n = 16). The strength of the FV-short bands varied in the affected plasmas. The FV-FL band also demonstrated interindividual intensity variation, but no systematic difference between affected and unaffected individuals. Note that it is not possible to judge the relative concentrations of the 2 FV forms in the affected individuals' plasma from the immunoblot analyses due to possible differences in transfer efficiencies.

The FV-short was found to be enriched by aluminum hydroxide ($Al[OH]_3$) absorption. Both FV-FL and FV-short were detected in the eluate; the FV-short band was strong in samples from affected individuals and barely detectable in those from unaffected individuals (Supplemental Figure 3A). The FV-short band, which was weakly visible after standard Coomassie staining (Supplemental Figure 3B), was analyzed by HPLC-TOF MS/MS, which accredited 3 peptides within the light chain of FV to this FV-short band (Supplemental Figure 4). The first peptide is located in the A3 domain and spans amino acids 1650–1659. The other 2 peptides are located in the C1 domain and span amino acids 1970–1982 and 2020–2039.

FV-short, the result of a factor V exon 13 splice variant. The association of the *F5* A2440G variant with the presence of a shortened form of FV in the plasma (FV-short) that reacts to the heavy chain–specific antibody AHV-5146 and contains peptide sequences of the A3 and C1 domain of FV by HPLC-MS/MS analysis led us to examine the *F5* transcript for splicing abnormalities involving exon 13, which encodes the B domain. RT-PCR of RNA from unaffected family members' white blood cells demonstrated a predominant transcript of expected size of 2946 bp based on the primers, along with a minor, smaller band at 840 bp. In contrast, the predominant transcript in affected patients' RNA was the 840 bp, and when sequenced, it was found to have base pairs 2441 through 4546 deleted (Figure 2). Thus, this *F5* genomic variant results in an in-frame deletion of 2106 base pairs that encode amino acids 756–1458 of the B domain of FV, most likely due to the use of what we believe to be a novel splice donor and acceptor site in the transcript (Figure 2B). Consequently, the abnormal transcript is predicted to encode a FV that has 702 amino acids deleted in the B domain and an insertion of an aspartic acid at the deletion site in affected individuals. Normal individuals producing this splice variant would have an asparagine residue at this deletion site. We devised a RT-PCR strategy to specifically amplify this novel splice variant and

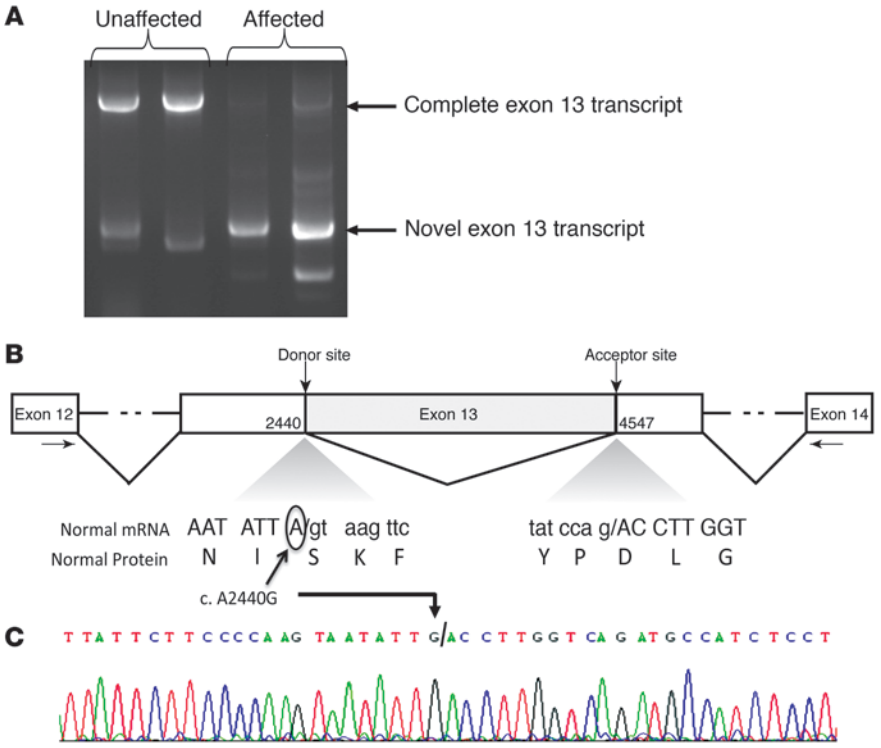

Figure 2

RT-PCR and diagram of novel splicing event in exon 13 of factor V. (**A**) Evaluation of exon 13 splice variants in unaffected and affected family members. Reverse transcription of 1 μg of RNA was completed using Superscript II RNase H- Reverse Transcriptase and oligo dT primer. cDNA was PCR amplified using Ex Taq Polymerase and primers F5e13F and F5e13R (indicated by arrows in **B**). The 2 left lanes show normal, unaffected RNA RT-PCR; the 2 right lanes show RNA from affected individuals. (**B**) Diagram of splicing event. Pre-mRNA of FV-short created by a splicing donor site at position 2441 and an acceptor site at position 4547 of exon 13 of the coagulation *F5* gene. This event results in the in-frame removal of 2106 coding base pairs from exon 13 that encode amino acids 756–1458. In this process, a new asparagine or aspartic acid residue would be created at this junction in normal or affected individuals, respectively. The sequence surrounding the splice site is separated into codons that encode wild-type FV with the corresponding normal protein sequence, and the splice sites are indicated by a backslash. This mutation changes the 5′ splice site from TA/GT to TG/GT. Diagram of gene is not to scale. (**C**) Sequencing results of the RT-PCR from affected patient RNA depicting the expression of A2440G in the splice donor site. These results are derived from the transcript-specific RT-PCR product (seen in Figure 3A) of an affected patient using FVShortF and FVShortR primers.

validate its expression in normal controls and in the liver, which is the primary source of the FV found in the bloodstream (12). Sequencing of this transcript-specific RT-PCRs of individuals with *F5* A2440G mutation confirmed that this mutation is expressed (Figure 2C) and appears to be preferentially amplified, as the normal (A2440) allele is not visualized in the sequencing reaction. Figure 3A confirms that this FV-short transcript is present in the RNA from unaffected individuals and in RNA from a control liver. Quantitative real-time PCR confirmed that FV-short transcript expression levels in individuals with A2440G ($n = 3$) were increased by an average of 22-fold ($P < 0.02$) compared with controls ($n = 3$) (Figure 3B), with considerable interindividual variation in expression levels of the FV-short transcript among the 3 affected individuals. Total *F5* transcript levels assessed using a commercial assay spanning the exon 12 and 13 splice junction did not significantly differ between patients and controls (data not shown).

Quantification of FV variants in plasma of family members. The concentrations of total FV and FV-FL were assessed in affected individuals ($n = 16$) with ELISAs using detecting antibodies against the light chain (HV1) or the B domain (MK30), respectively. The total FV and FV-FL concentrations (mean ± SD) were 25.6 ± 4.9 nM and 20.7 ± 4.1 nM, respectively. Corresponding values of an unaffected pool were 22.7 and 21.3 nM, respectively. The concentration of FV-short in individual affected family members (estimated by subtracting the MK30 ELISA values from those of the HV1 ELISA) demonstrated considerable interindividual variation, 4.8 ± 2.0 nM mean ± SD (range 1.7–8.4 nM).

Presence of coagulation inhibitor in affected patient plasma. A thrombin generation assay (TGA) was used to evaluate the extrinsic coagulation pathway in plasma from individual family members. All affected family members carrying the *F5* mutation demonstrated decreased thrombin generation with prolonged lag phase (mean ~12 minutes vs. ~4 minutes in unaffected) as well as decrease in peak heights and area under the curves (Figure 4). Mixing affected and unaffected plasma at increasing ratios demonstrated gradually increased inhibition of thrombin generation with prolonged lag phases and decreased peak heights, suggesting that affected plasma contains a coagulation inhibitor (Figure 4). The delayed thrombin generation correlated to slow activation of both FV-FL and FV-short in affected plasma, as visualized by the slow production of both heavy and light FVa chains (Figure 5, B and C, respectively).

Inhibitory activity associated with FV-short in affected plasma. To elucidate whether the inhibitory activity present in affected plasma was associated with FV-short, the plasma was subjected to immunodepletion using polyclonal FV antibodies and then tested in the TGA after addition of recombinant FV-FL (rFV-FL) or rFV-short. FV depletion completely blunted the thrombin generation in both affected and unaffected plasma. The addition of either rFV-FL or rFV-short to the FV-depleted plasmas resulted in normal thrombin generation in both affected and unaffected plasma (Figure 6). These results demonstrated that the inhibitory activity was directly associated with FV in the affected plasma and was removed by immunodepletion. Selective immunodepletion of the FV-FL with a B domain monoclonal antibody (MK30) demonstrated that the inhibitor was specifically associated with FV-short in affected plasma because the inhibitory activity remained in the FV-FL–depleted plasma (Figure 7).

The FV-short–associated inhibitor in affected patient plasma identified as TFPIα. The results presented above suggested the possibility that the FV-short–associated inhibitory activity was not an intrinsic property of FV-short itself, but caused by an inhibitor that was

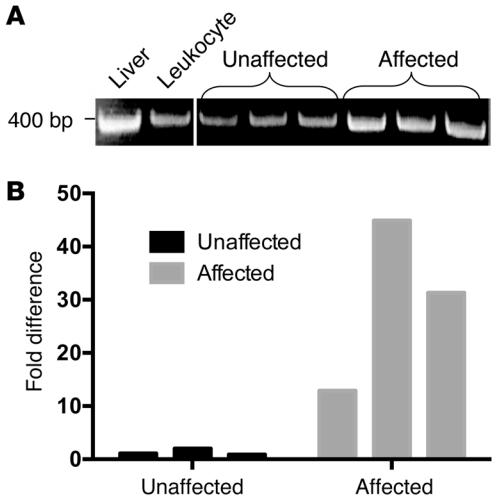

Figure 3
Analysis of the expression of FV-short alternative splicing variant in affected patients. (**A**) Transcript-specific reverse transcription of 1 μg of RNA was completed using Superscript II RNase H- Reverse Transcriptase and FVShortR primer. cDNA was PCR amplified using Ex Taq Polymerase and FVShortF and FVShortR primers. Lane 1: unaffected liver RNA RT-PCR; lane 2: normal peripheral leukocyte RNA; lanes 3–5: unaffected patient RNA RT-PCR; lanes 6–8: affected patient RNA RT-PCR. The lanes were run on the same gel but were noncontiguous. (**B**) Quantitative real-time PCR of FV-short transcript was completed using a custom TaqMan assay. Fold difference of FV-short expression in unaffected controls (n = 3) compared with affected patients (n = 3). Fold differences are normalized to 18S expression and relative to corresponding target expression in normal peripheral leukocyte RNA. The 1-tailed P value calculated using the Student's t test was 0.02.

associated with FV-short in affected plasma. As TFPIα has been shown to interact with FV in normal plasma (24, 27), individual plasmas from family members were analyzed by immunoblotting using an antibody against the N terminus of TFPI (AHTFPI-5138) (Figure 8). All affected individuals demonstrated a very strong TFPI immunoreactive band at 40 kDa, whereas the corresponding TFPI band in unaffected family members was barely detectable. This observation was further confirmed using a rabbit monoclonal antibody against the C terminus of TFPIα, which yielded a similarly strong band in affected plasma (Supplemental Figure 5). The rTFPIα migrated at a slightly higher molecular weight position than plasma TFPIα, most likely due to glycosylation differences, as the migration of the 2 was similar after deglycosylation with N-glycosidase F (Supplemental Figure 5). A dilution series of recombinant TFPIα analyzed by immunoblot analysis (not shown) semi-quantitatively estimated the TFPIα concentration to be approximately 5 nM in the affected plasma pool and less than 0.5 nM in the unaffected plasma pool. Three different ELISA variants against TFPI were used to estimate the concentrations of the different isoforms of TFPI. The first ELISA measuring total TFPI, using polyclonal anti-TFPI as catcher and a monoclonal antibody against Kunitz 1 as detector, demonstrated that affected family members' plasma contained 5.3 ± 1.2 nM (mean ± SD) TFPI, whereas a pool of unaffected plasma contained 1.4 nM TFPI. The second ELISA recognizing TFPIα, using the same polyclonal as catcher and a monoclonal antibody against Kunitz 3 as detector, suggested the TFPIα concentration to be 2.5 ± 0.7 nM in affected family members and 0.36 nM in the unaffected pool. The third ELISA (Asserachrom Free TFPIα; Stago), using a monoclonal antibody detecting all TFPI isoforms as catcher and a monoclonal antibody against the C terminus as detector, measured 1.25 ± 0.7 nM TFPIα (mean ± SD) in affected family members and 0.14 nM in the unaffected plasma pool. To prove that the high concentrations of TFPIα in plasma of affected family members caused the inhibition in the TGA, polyclonal antibodies were added to affected plasma prior to the TGA. This resulted in complete normalization of the TGA (Figure 9A). Furthermore, addition of increasing concentrations of rTFPIα to unaffected plasma resulted in a dose-dependent inhibition of thrombin generation, yielding curves similar to those of plasma from affected individuals (Figure 9B).

Complexes between FV-short and TFPIα in plasma. Our results suggested that TFPIα was specifically associated with FV-short in plasma of affected family members. This was validated when immunodepletion using polyclonal TFPI antibodies removed most of FV-short, while leaving FV-FL, in the TFPI-depleted plasma (Figure 10, A and B). FV-short was recovered in the TFPI immunoprecipitate. The conclusion that TFPIα was specifically associated with FV-short gained additional support from immunodepletion experiments using HiTrap columns coupled with either the B domain monoclonal antibody MK30 or an Ig fraction of the polyclonal FV antiserum #8806 (Figure 10, C and D). MK30 specifically removed FV-FL from plasma, leaving both FV-short and TFPIα in the immune-absorbed plasma. In contrast, the polyclonal FV antibodies immunodepleted FV-FL and FV-short as well as TFPIα.

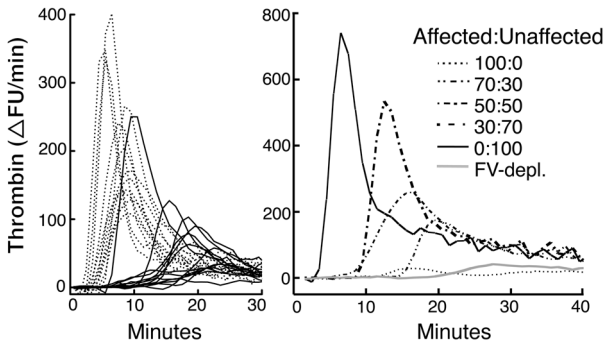

Figure 4
TF-induced TGAs of plasma from affected and unaffected family members. Individual thrombin generation curves are shown to the left. Affected family members are represented by solid lines, whereas the unaffected individuals are denoted with dotted lines. The affected individual with the highest thrombin generation was individual IV:17, who, in the Western blotting (Figure 1), demonstrated a weak FV-short band. The thrombin generation was monitored using fluorogenic substrate I-1140, the thrombin concentration given as Δ FU/ml (FU, fluorescence units). The right part of the figure demonstrates the thrombin generation using mixtures of affected and unaffected pooled plasma.

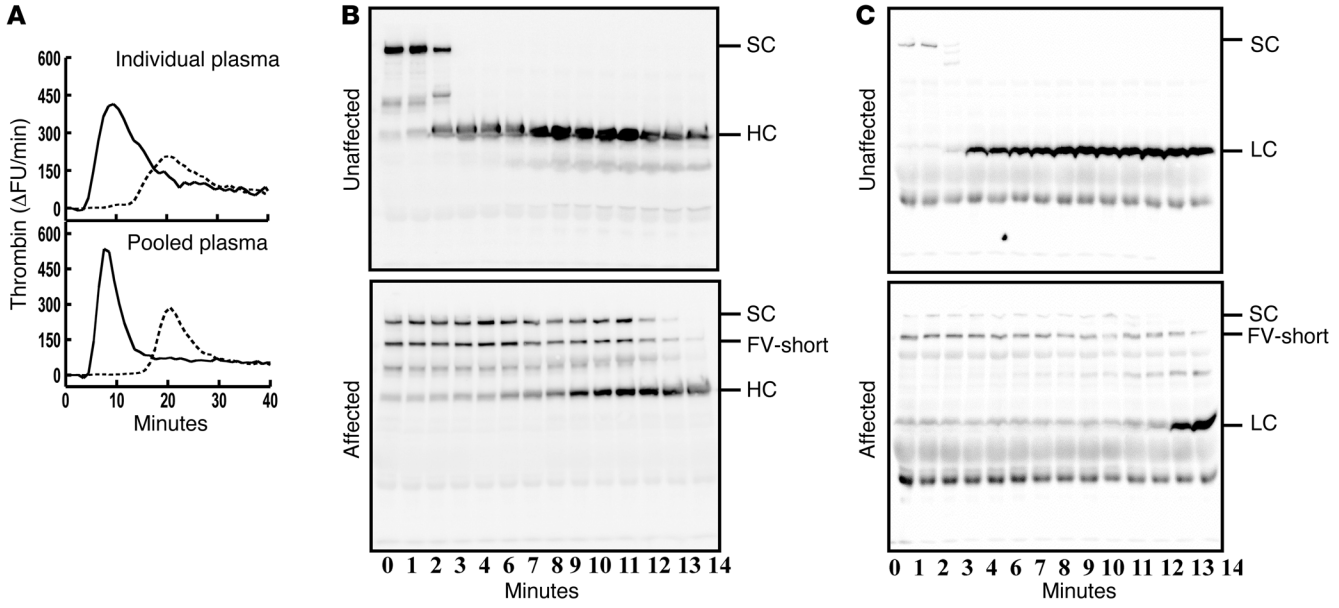

Figure 5
Slow FV activation in affected patient plasma during TGA. (**A**) Thrombin generation of unaffected (solid line) and affected patient samples (dashed line) as individual (top) and pooled (bottom) plasmas. (**B** and **C**) Immunoblot analyses of the activation of FV into its heavy (**B**) and light (**C**) chains in unaffected (top) and affected (bottom) patient pooled plasma during thrombin generation. FV was detected using AHV-5146 (**B**) against the heavy chain and AHV-5112 (**C**) against the light chain, and Supersignal West Dura Extended Duration Chemiluminescence substrate was used to develop the Western blots. SC, wild-type FV single chain; HC, heavy chain of active FV; LC, light chain of active FV.

Plasma from unaffected individuals was also found to contain the TFPIα:FV-short complexes but at much lower concentrations. This was evident when TFPI immunoprecipitates from larger volumes of normal versus affected plasma (5 ml vs. 0.3 ml) were analyzed by immunoblotting for FV and TFPI (Figure 10, E and F). It is noteworthy that the immunoprecipitate from normal plasma also contained FV-FL. According to the Image Lab analysis tool, the FV-short and FV-FL band signals were similar in strength, suggesting TFPIα in normal plasma to be approximately equally distributed between the 2 isoforms of FV.

TFPIα binds with higher affinity to FV-short than to full-length FV. The results presented above suggest that TFPIα binds with higher affinity to FV-short than to FV-FL. To verify this hypothesis, rTFPIα was incubated with mixtures of rFV-short and FV-FL at different concentrations, including conditions chosen to mimic the situation in unaffected and affected plasma. The mixtures were subjected to immunoprecipitation using the AHTFPI-S antiserum bound to magnetic beads and the supernatants and immunoprecipitates were analyzed by immunoblotting using monoclonal antibodies to FV (AHV-5146) and TFPI (AHTFPI-5138) (Figure 11). rTFPIα was found to preferentially bind to rFV-short even when FV-FL was present in molar excess, demonstrating that the binding affinity of TFPIα for FV-short is higher than for FV-FL.

Discussion

Patients affected by the east Texas type bleeding disorder exhibit mild prolongations of their APTT and/or PT, but have bleeding episodes indicative of a moderately severe disease (28). Although their FV levels and activities clinically measure as normal, we provide evidence that the A2440G mutation in the B domain exon 13 of the *F5* gene causes the bleeding disorder through an indirect gain-of-function mechanism. In affected individuals, the mutation increases the use of an alternative splice donor site in exon 13 and increases the production of an alternative isoform of FV. This isoform encodes a shortened FV with an in-frame 702 amino acid deletion in the B domain, deemed FV-short. FV-short indirectly inhibits coagulation by forming a high-affinity complex with the coagulation inhibitor TFPIα. As a result of the association with FV-short, TFPIα concentrations in plasma of affected family members are dramatically increased, presumably due to the retention in circulation of the complex of FV-short and TFPIα. This is the first description, to our knowledge, of an autosomal dominant bleeding disorder associated with a gain-of-function mutation in the *F5* gene. Additionally, this is the first known bleeding phenotype resulting from increased plasma levels of TFPIα.

Our extensive evidence demonstrates that FV-short is the result of alternative splicing and not due to aberrant proteolytic cleavage. The FV-short isoform reacted with both the monoclonal antibody AHV-5146, which has its epitope between residues Arg-306 and Arg-506 in the heavy chain of FV (31), and the monoclonal antibody AHV-5112 against the light chain. In contrast, the B domain–specific monoclonal antibody MK30 does not recognize FV-short. HPLC-TOF MS/MS analysis of the partially purified FV-short indicated the presence of peptide sequences found in domains A3 and C1 of FV. Given these findings and the fact that the light chain is only approximately 74 kDa, there are no possible proteolytic cleavages that can account for the loss of approximately 80 kDa of protein observed for FV-short. Instead, our results support the conclusion that a splicing event in exon 13 occurs normally to a low degree in controls and the efficiency of this splicing event is increased by the presence of the A2440G mutation. However, the essentially normal levels of circulating

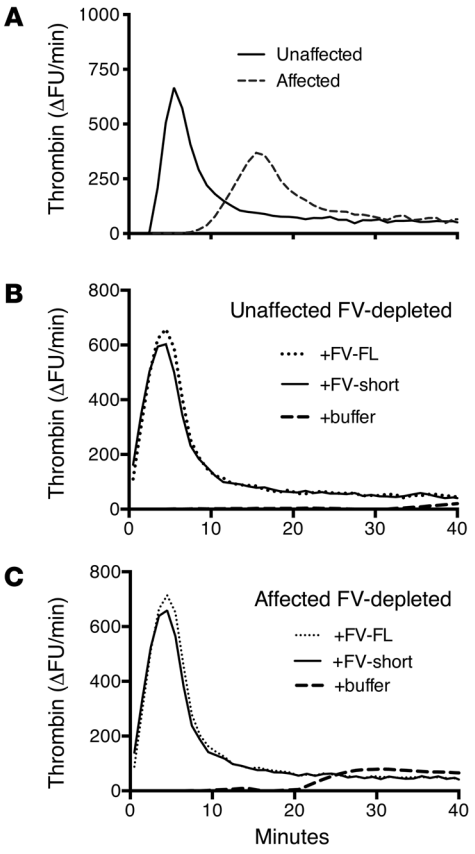

Figure 6
TGA after factor V depletion/reconstitution. (**A**) TGAs of unaffected (solid line) and affected patient samples (dashed line). Unaffected (**B**) and affected plasma (**C**) were subjected to FV immunodepletion using a polyclonal antibody against FV (#8806) that was covalently coupled to a 1-ml HiTrap column. Due to the FV depletion, thrombin generation was completely abolished (dashed lines in **B** and **C**). Upon the addition of 2 nM recombinant FV-FL or FV-short, both plasmas exhibited similar, normal thrombin generation.

FV-FL in affected individuals suggest that the mutant allele is only partially spliced at this site. The concentration of circulating FV-short in affected family members is consistently elevated, but the variation among individuals in its levels suggests variation in the splicing efficiency at this site also exists among affected individuals. We were unable to obtain RNA samples on all affected individuals to directly correlate this transcript expression to the protein differences observed in their plasma. FV-short was not observed in direct plasma immunoblots of unaffected individuals, but was observed in partially purified FV extracts of plasma (Supplemental Figure 3A), suggesting that low levels of FV-short are present in normal individuals. Moreover, immunoprecipitation of larger volumes of unaffected plasma as compared with affected plasma with antibodies against TFPI demonstrated the presence of TFPIα:FV-short complexes in addition to TFPIα:FV-FL complexes. Thus, in normal healthy individuals, TFPIα circulates in complex with either FV-short or FV-FL.

TFPIα in normal plasma is reported to interact with FV, and depletion of FV results in an 80% decrease in TFPIα levels (24). The affinity between normal FV and TFPIα was suggested to be relatively low, and half-maximum binding of FV to immobilized TFPIα in surface plasmon resonance analysis was observed at 13.5 nM (24). Under normal conditions, the plasma concentration of FV (≈20 nM) is approximately 50- to 100-fold higher than the plasma concentration of TFPIα (≈0.2 nM), suggesting that only a minor fraction of circulating FV-FL carries a TFPIα molecule. We now demonstrate that low levels of FV-short in normal plasma also bind TFPIα, but the normal distribution of TFPIα between the 2 FV isoforms remains to be elucidated. The situation in affected family members dramatically differs with the presence of much higher concentrations of the FV-short isoform, all of which circulate in complex with TFPIα, as judged by immunoprecipitation. Likewise, most or all of TFPIα in affected plasma is associated with the FV-short form. We currently have no direct, specific method to accurately determine the concentration of FV-short, but we estimated the mean FV-short concentration to be 4.8 nM in affected individuals using 2 ELISAs, one determining the total FV and the other FV-FL, with the difference attributed to the presence of FV-short. The total TFPI concentration in affected plasma was measured to be 5.3 nM and in unaffected plasma 1.4 nM. The 2 ELISA assays for TFPIα isoforms using detecting monoclonal antibodies either against Kunitz 3 or the C terminus yielded 2.5 nM and 1.25 nM TFPIα in affected plasma, respectively. Corresponding values in unaffected plasma were 0.36 and 0.14 nM. The difference between the 2 TFPIα assays is compatible with the observation that approximately half of TFPIα in plasma is truncated in the C terminus (25). From these numbers it is difficult to accurately estimate the stoichiometry between FV-short and TFPIα in affected plasma, but the results are compatible with a 1:1 stoichiometry. Our results also suggest that the affinity of the TFPIα:FV-short interaction in affected plasma is considerably higher than that between FV-FL and TFPIα and that TFPIα preferentially binds to the FV-short isoform despite a molar excess of FV-FL. This hypothesis gained experimental support when recombinant FV-short and FV-FL were allowed to compete for rTFPIα, and even when FV-FL was present at molar excess, TFPIα preferentially bound FV-short over FV-FL. This taken together with the pres-

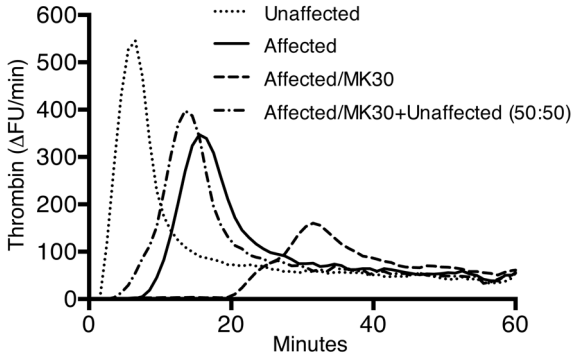

Figure 7
Inhibitor remaining after depletion of FV-FL. Pooled plasma was subjected to immunodepletion using a 1-ml HiTrap column with MK30, which specifically depleted FV-FL, leaving FV-short in the supernatant (see Figure 10). The immunodepleted plasma was subjected to TGA, either alone or after mixing with unaffected plasma.

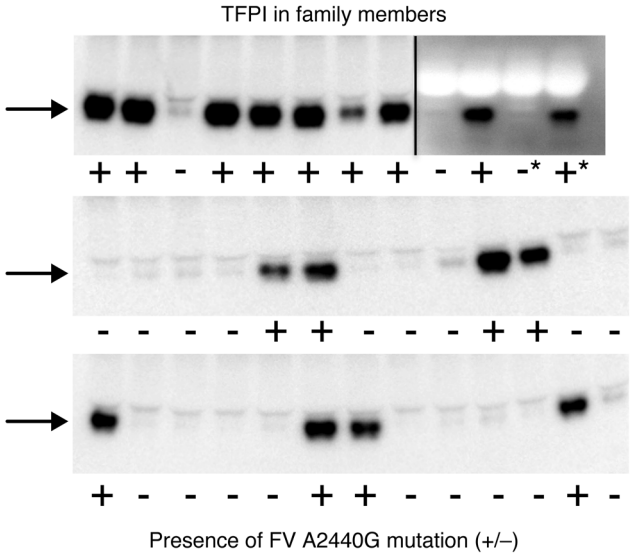

Figure 8
High TFPI concentrations in plasma of affected family members. Immunoblot analysis of plasma (equivalent to 0.5 μl) from affected and unaffected family members, with TFPI being detected using the monoclonal AHTFPI-5138 against Kunitz 1 in combination with HRP-conjugated goat anti-mouse antiserum and developed with chemiluminescence. The SDS-PAGE (4%–15%) was run under nonreducing conditions. Lanes marked with plus signs represent affected individuals carrying the A2440G mutation, whereas those marked with minus signs represent unaffected family members. The arrows point at the approximately 40-kDa TFPIα band. The 2 lanes in the upper row that are marked with asterisks represent pools of unaffected (–*) and affected (+*) family members. The 4 right lanes in the upper row were derived from a immunoblot separate from those shown on the 8 lanes to the left. Note the weak TFPI band in the seventh sample from the left in the upper row, the sample being derived from individual IV:17 in family pedigree (Supplemental Figure 1).

ence of TFPIα:FV-short complexes in normal plasma supports the conclusion that FV-short binds with higher affinity than FV-FL, as the concentration of FV-short in normal plasma is approximately 20-fold lower than that of FV-FL.

Ndonwi et al. (27) recently reported that the binding site in TFPIα to both FV and FVa is located in the last 25 C-terminal amino acids of the protein, a region that contains a highly positively charged cluster of lysines and arginines. This fact taken together with the ionic nature of the interaction suggests that the binding site for TFPIα in FV/FVa should be a highly negatively charged region. There are several such areas in FV/FVa, including the region upstream of the thrombin cleavage sites at positions 709 and 1545. Further studies will determine the details of the TFPIα binding to normal FV/FVa and to FV-short and address the question as to why TFPIα preferentially binds the FV-short isoform rather than the FV-FL. A recent paper by Bos and Camire (32) reported that 2 regions in the B domain are important to keep FV in a procofactor state — one being positively charged (963–1008) and the other, close to the 1545 thrombin-cleavage site (1493–1537), being negatively charged. Deletions in recombinant FV of either the basic or the acidic cluster yielded FV in an active state. According to the hypothesis proposed by Bos and Camire, the 2 regions bind to each other in intact FV and thus maintain FV in its procofactor form. This potentially unbalanced acidic region (1493–1537) in the B domain of FV-short may be involved in creating a high affinity binding site for TFPIα.

TFPIα is a relatively low molecular weight protein (≈40 kDa) and unless bound to a carrier would be eliminated by filtration in the kidneys. Presumably the binding of TFPIα to FV-short in affected family members' plasma results in its retention in circulation, thus causing the higher TFPIα plasma concentrations. Even though the concentration of TFPIα in plasma is normally very low, significant amounts are present in the vasculature associated with the endothelium (25, 26). Infusion of heparin releases part of the TFPIα from the endothelium to the circulation. Possibly, the FV-short

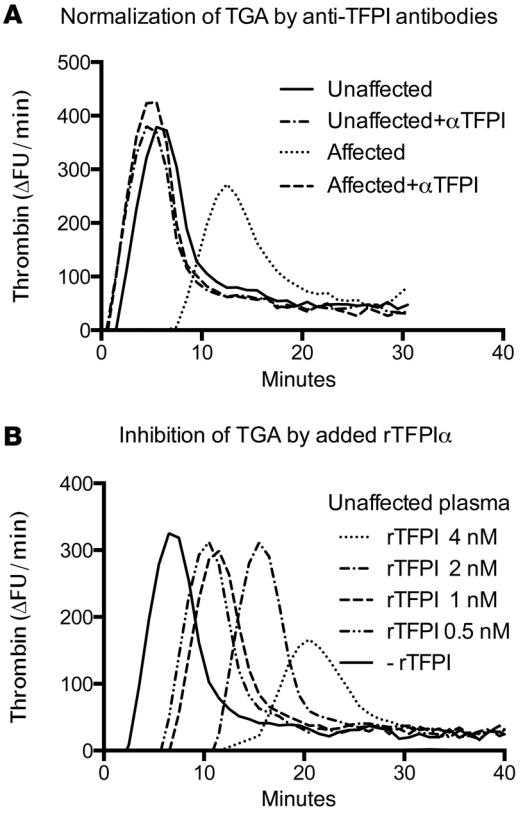

Figure 9
Normalization of thrombin generation in affected plasma by anti-TFPI and effects of adding TFPIα to unaffected plasma. (**A**) Polyclonal antibodies against TFPI (40 μl; final concentration of 100 μg/ml) or 40 μl HNBSA buffer control were mixed with 40 μl pooled plasma from affected or unaffected family members, and after 5 minutes incubation at 37°C, the TGA was started by addition of substrate (20 μl) and TF/PL/Ca^{2+} mixture (20 μl). (**B**) Increasing concentrations of rTFPIα (in 8 μl) were added to unaffected plasma (72 μl), yielding the indicated final concentrations, and tested in the TGA. A dose-dependent prolongation of the lag phase was observed, the highest TFPI concentration also decreasing the thrombin peak.

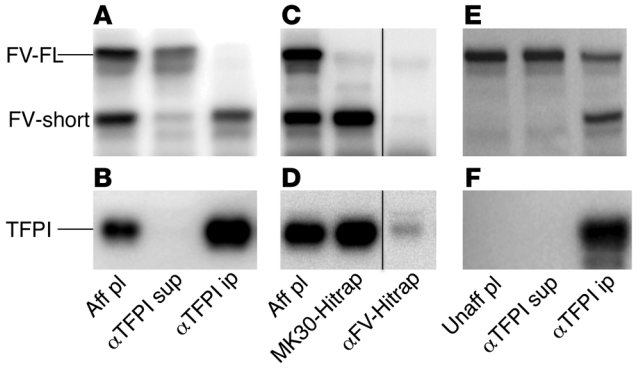

Figure 10
TFPIα:FV-short complexes in plasma. (**A**–**D**) A pool of plasma from affected family members was subjected to either FV or TFPI depletion to analyze whether TFPI was specifically associated with FV-short. (**A** and **B**) Plasma (300 μl) was incubated with 900 μl Streptavidin-coated magnetic beads carrying biotinylated polyclonal antibodies against TFPI (AHTFPI-S). After 2 hours at 11°C, the mixture was centrifuged, the supernatant diluted 1:40 in sample preparation buffer, and 10 μl added for Western blot analysis using a monoclonal antibody against FV (**A**, AHV-5146) or an antibody against TFPI (**B**, ATFPI-5138 against Kunitz 1 domain). The beads were washed once in HNSBSA and bound TFPI eluted with 300 μl sample preparation buffer; 10 μl of a 1/20 dilution was loaded and analyzed with antibodies against FV (**A**) and TFPI (**B**). Aff, affected; sup, supernatant, ip, immunoprecipitate (**C** and **D**) Affected plasma (1 ml) was either loaded to a 1-ml HiTrap column with coupled MK30 against the FV B domain or a 1-ml HiTrap column with coupled polyclonal anti-FV IgG (#8806) (αFV). After 30 minutes incubation, the plasma was eluted and analyzed by Western blotting for FV (**C**) or TFPI (**D**). The lanes in **C** and **D** were run on the same gel but were noncontiguous. (**E** and **F**) Unaffected plasma (5 ml) was immunoprecipitated with 1 ml anti-TFPI magnetic beads, essentially as in **A** and **B**. The starting plasma and the supernatant (10 μl of 1/10 dilution) were analyzed with antibodies against FV (**E**, AHV-5146) or TFPI (**F**, ATFPI-5138). The beads were washed and eluted with 100 μl sample preparation buffer, and 10 μl undiluted sample was analyzed for FV (**E**) and TFPI (**F**).

form competes with the endothelial binding, which together with retention in the circulation of TFPIα by FV-short, could explain the increased plasma concentrations of TFPIα.

It is noteworthy that the clinical levels and activities of FV and the other coagulation factors in our patients measured as normal despite the high concentrations of the inhibitory FV-short–TFPIα complexes. Presumably, this is the result of the dilutions of patient plasma made in the assays, and this dilution in combination with the use of high amounts of TF in the routine tests, which generates high concentrations of FVIIa and FXa, overcomes the inhibitory activity of the TFPIα. In contrast, the TGAs were performed at low plasma dilution and in the presence of small amounts of TF and were therefore directly influenced by the TFPIα:FV-short complexes in affected individuals. The prolongation of the APTT observed in affected individuals suggests that the TFPIα:FV-short complexes are also efficient in inhibiting FXa when generated by the intrinsic pathway. In agreement with this, we found that an intrinsic pathway-specific TGA was also pathological when affected plasma was tested (results not shown).

In conclusion, we have identified what we believe is the first autosomal dominant bleeding disorder due to a gain-of-function mutation in the gene encoding coagulation FV. The mutation upregulates a previously unidentified alternatively spliced transcript of *F5*. The resultant isoform, FV-short, was present at much higher levels in A2440G carriers' plasma versus noncarriers' plasma. FV-short causes the bleeding phenotype by binding and retaining TFPIα in circulation, therefore leading to higher plasma concentration of TFPIα. The identification of TFPIα as the active inhibitory compound in the affected family members opens possibilities for future therapeutic intervention in the affected family members, as TFPI inhibitors are presently under development (33).

Methods

Family characterization and specimen collection. The family spans over 4 generations and has 22 known affected members (Supplemental Figure 1). Clinical descriptions and assessment of this family have been previously described (28). Whole blood from 3.2% (0.105 M) sodium citrate blood collection tubes or blood bags with anticoagulant citrate phosphate dextrose adenine solution, USP (BD) was centrifuged at 3000 *g* for 10 minutes. Plasma was removed, frozen on dry ice, and stored at –80°C.

Partial purification of FV-short and mass spectrometry. The FV-short was enriched by $Al(OH)_3$ absorption and elution (34). HPLC-TOF MS/MS was performed at the Proteomics Core Laboratory at the University of Texas Health Science Center at Houston (UTHSC-H). Normal plasma FV was purified as described (35).

Electrophoretic analysis. SDS-PAGE analysis was performed using standard techniques. For Western blotting, 4%–15% gradient SDS-PAGE gels (Bio-Rad) were used. The proteins were transferred to PVDF membranes (Bio-Rad), and visualized with monoclonal AHV-5146 against the heavy chain (Haematologic Technologies Inc.) or the monoclonal AHV-5112 (Haematologic Technologies Inc.) against the light chain. To detect the B domain, MK30 (in house) was used. TFPIα was visualized using a monoclonal antibody against the N terminus of TFPI (AHTFPI-5138; Haematologic Technologies Inc.) or against the C terminus with a rabbit monoclonal antibody (clone EPR7941; Epitomics). Final detection was completed with horseradish peroxidase–conjugated appropriate secondary antibody and the Supersignal West Dura Extended Duration Chemiluminescence Substrate (Pierce), monitored with a Fuji LAS 3000IR CCD camera, analyzed with Image-Gauge or with the ChemiDoc Imaging System from Bio-Rad, and quantified with Image Lab software.

Reverse transcription and real-time PCR. Standard oligonucleotides were purchased from Integrated DNA Technologies or DNA Technologies. Total blood RNA was obtained using PaxGene Blood RNA Collection Kit per the manufacturer's instructions (QIAGEN). Quality and concentration of RNA was assessed using an Agilent 2100 Bioanalyzer (Agilent Technologies) at the UTHSC-H Quantitative Genomics Core Laboratory. Reverse transcription of 1 μg of RNA derived from whole blood of unaffected and affected family members, control liver (Ambion), or leukocyte RNA (Clontech) was performed using an oligo-dT or *F5* gene-specific primer, F5ShortR, (5′-TGGAGGAGTTGATGTTTGTCC-3′) with Superscript II RNase H^- Reverse Transcriptase (Invitrogen) in a total volume of 100 μl according to the manufacturer's instructions. Exon 13 splice variants were amplified using the primers F5e13F (5′-CATGCGTGGAGAATCTGTGACGGT-3′) and F5e13R (5′-GTGCTGTCGAGGTACTTTCG-3′) in a 20-μl reaction containing 2 μl of oligo-dT reverse-transcribed RNA, 0.025 U/μl Ex Taq Polymerase (Takara), 1× PCR buffer, and 0.15 mM dNTPs (Invitrogen). The PCR was initiated at 94°C for 2 minutes, amplified with 35 cycles of 30 seconds at 94°C, 45 seconds at 55°C, and 7 minutes at 68°C, and contained a final elongation for 10 minutes at 68°C.

The FV-short splice variant was specifically targeted for amplification using 0.25 μM of the aforementioned reverse primer FVShortR and a for-

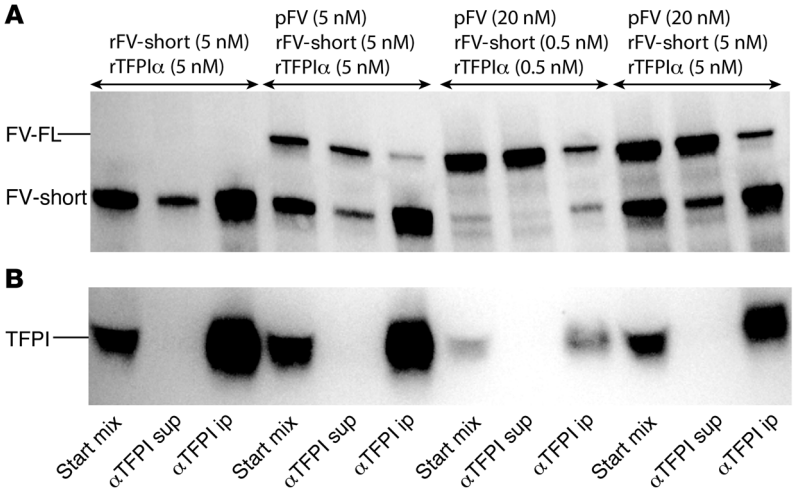

Figure 11
TFPIα preferentially binds to FV-short. Mixtures of rTFPIα (0.5 or 5 nM) and rFV-short (0.5 or 5 nM) ± plasma-derived FV (5 or 20 nM) were incubated overnight in a total volume of 100 μl and then subjected to immunoprecipitation with Streptavidin-coated magnetic beads (300 μl) carrying biotinylated polyclonal antibodies against TFPI (AHTFPI-S). The bead pellets were eluted with 33 μl sample preparation buffer, 10 μl being loaded to the gel. The pellets, the start mixes, and the supernatants (1 μl each) were analyzed by immunoblotting for (**A**) FV (AHV-5146) and (**B**) TFPI (AHTFPI-5138).

ward primer, FVShortF, with sequence 5′-CGGAAAATGCATGATCGTT-3′ in the same 20-μl PCR reaction mentioned above, with the exception of the use of 2 μl of *F5* gene-specific reverse-transcribed RNA in lieu of the oligo-dT cDNA. The PCR was initiated at 94°C for 1 minute, amplified with 35 cycles of 10 seconds at 94°C, 20 seconds at 55°C, and 20 seconds at 72°C, and contained a final elongation for 2 minutes at 72°C. PCR products were sequenced using BigDye Terminator v3.1 chemistry and ABI 3130xl Genetic Analyzer (Applied Biosystems).

For real-time PCR, reverse transcription of 1 μg of affected (n = 3) and unaffected (n = 3) patients and control peripheral leukocyte RNA in a reaction volume of 100 μl was performed using each transcript-specific primer: total *F5* (5′-CAAGAGTAGTTATGCTCTCAGGC-3′), eukaryotic 18S ribosomal RNA (5′-CCTAGCTGCGGTATCCAGGC-3′), and FV-short (5′-TGGAGGAGTTGATGTTTGTCC-3′). Real-time RT-PCR analysis of reverse transcripts was performed with the ABI Prism Sequence Detection System 7700 using TaqMan Reaction Master Mix and TaqMan Gene Expression Assays Hs00914105_m1 for total human *F5*, which spans the exon 12/13 splice junction, and Hs99999901_s1 for eukaryotic 18S ribosomal RNA (Applied Biosystems). In addition, a custom TaqMan assay for FV-short splicing transcript was produced with the following specifications: hFV-short(+): 5′-TTCAAATTATTCTTCCCCAAGT-3′, hFV-short(–): 5′-AGAAAAGTATCATTGAGAGTAGGAGA-3′, hFV-short(+)FAM/MGB probe: 5′-ACCTTGGTCAGATGCCATCTCCTTC-3′ (Applied Biosystems). The real-time reaction consisted of 5 μl of cDNA, 5 μl of reaction Master Mix, and 0.5 μl of each expression assay. cDNA for 18S was diluted 1:500 to avoid saturation of the real-time assay. The real-time PCR initiated at 95°C for 5 minutes, followed by 50 cycles of 10 seconds at 95°C and 30 seconds at 58°C. FV-short and total *F5* expression were normalized to eukaryotic 18S ribosomal RNA and analyzed relative to control leukocyte RNA (Clontech).

Production, expression, and quantification of FV recombinants. A pMT2 vector containing the full-length cDNA of human *F5* (pMT2-FV) was used as a template for creating the mutant recombinant expression vector. Recombinant wild-type and mutant vectors were transiently transfected into COS1 cells using the diethyl aminoethyl-dextran (DEAE-dextran) method essentially as described previously (36–38). The details of the mutagenesis and expression are described in the Supplemental Methods. In brief, the A2440G (GenBank M16967) mutation that would result in a serine-to-glycine change at amino acid 756 (FV-S756G) was created using the QuikChange site-directed mutagenesis kit (Stratagene). The splice variant mutant vector (FV-702 or rFV-short) was created by cloning in an insert with A2440G and a deletion of base pairs 2441 to 4546 that correlate to the in-frame deletion of amino acids 756 through 1458. The recombinant proteins were harvested in serum-free medium (Optimem Glutamax; Gibco) and concentrated using 100,000 MWCO Vivaspin (GE Healthcare). Aliquots were stored at –80°C. Concentrations of the recombinant proteins were determined by a PTase assay and an ELISA as previously described (31).

TGA. Thrombin generation of normal and affected patient citrated plasma was initiated with TF (Dade Behring) (final concentrations of 1.4 or 2.8 pM as indicated in the figure legends), 10 μM PL vesicles (20:20:60 of phosphatidylserine (PS) (brain extract), phosphatidylethanolamine (PE) (egg extract), phosphatidylcholine (PC) (egg extract)) (Avanti Polar Lipids), and 16 mM of $CaCl_2$ and monitored through fluorogenic substrate I-1140 (Z-Gly-Gly-Arg-7-amino-4-methylcoumarin·HCl) from Bachem at a final concentration of 300 μM essentially as previously described (39).

Immunodepletion of FV variants and TFPI. To ensure results were directly correlated to FV, normal and affected patient plasma were subjected to immunodepletion using a polyclonal antibody against FV (#8806; 10 mg) with epitopes to the heavy and light chain as well as to the B domain that was covalently coupled to a 1-ml HiTrap N-hydroxysuccinimide–activated column (GE Healthcare). Plasma was adsorbed for 30 minutes at room temperature and eluted with TBS buffer (50 mM Tris, 150 mM NaCl, pH 7.5). FV depletion was confirmed by Western blotting and ELISA. Recombinant full-length FV (FV-FL) or FV-short (2 nM) was then added to the immunodepleted plasma, which was subsequently tested for thrombin generation. The FV-FL in affected plasma was specifically immunodepleted either using a HiTrap column with immobilized MK30 (essentially as described above) or alternatively by using a biotinylated MK30 coupled to streptavidin-coated magnetic beads (Dynal Biotech ASA), essentially as described previously (40). The influence of TFPIα on the thrombin generation was investigated by inhibiting TFPIα through the addition of an IgG fraction of sheep polyclonal antibodies (40 μl; 100 μg/ml final concentration) against TFPI (PAHTFPI-S; Haematologic Technologies Inc.) to plasma (40 μl). After incubation for 5 minutes at 37°C, 20 μl substrate was added followed by 20 μl of the TF/PL/Ca mixture to initiate the thrombin generation reaction. The effect of adding increasing concentrations of rTFPIα to unaffected plasma was also tested in the TGA.

Immunoprecipitation of TFPIa:FV-short complexes. TFPIα:FV-short complexes were immunoprecipitated using biotinylated AHTFPI-S immobilized to Streptavidin-coated magnetic beads (80 μg antibodies per ml bead slurry). Affected plasma (300 μl) were incubated at 4°C for 2 hours with beads from 900 μl slurry, whereas 5 ml unaffected plasma was used with 1000 μl bead slurry. The beads were collected, washed in 50 mM Hepes, 0.15 M

NaCl, pH 7.5, containing 1% BSA (HNSBSA), and dissolved in sample preparation buffer, 300 μl for affected and 100 μl for unaffected. The start plasma, the supernatants, and the eluted immunoprecipitates were analyzed by immunoblotting for FV and TFPIα (Figure 10).

Generation of rTFPIα:rFV-short complexes. Complexes between rTFPIα and rFV-short were formed by incubating the 2 proteins at equimolar concentrations (5 nM) in HNBSA containing 2 mM $CaCl_2$ (HNSBSA-Ca) overnight in the refrigerator. To investigate whether TFPIα preferred FV-short over FV-FL, TFPIα (0.5 or 5 nM) was incubated with mixtures of FV-short (0.5 or 5 nM) and FV-FL (5 or 20 nM) and then subjected to immunoprecipitation using AHTFPI beads, as described above. The start mix, the supernatants, and the immunoprecipitates were analyzed by immunoblotting for FV and TFPIα (Figure 11).

Determination of FV and TFPI variants by ELISA. B domain–containing full-length FV was determined with an ELISA using polyclonal rabbit anti-human FV (#8806) as catcher and the monoclonal B domain antibody MK30 as detector (41). To measure total FV (full-length plus FV-short), MK30 was replace by an antibody against the light chain of FV (HV1; Sigma-Aldrich). The concentration of total TFPI in plasma was determined with an ELISA in which a polyclonal TFPI antibody (PAHTFPI-S, Haematologic Technologies Inc.) was used as catcher and a monoclonal anti-TFPI against the N terminus (AHTFPI-5138; Haematologic Technologies Inc.) as detector. To measure TFPIα, 2 different ELISAs were used. The first used a polyclonal TFPI antibody (AHTFPI-S) as catcher and a monoclonal antibody against the third Kunitz domain (MBS532509l clone M105273 from MyBiosource) as detector. The assays were standardized with purified recombinant full-length TFPIα, provided by T. Hamuro (Chemo-Sero-Therapeutic Research Institute, Kaketsuken, Kumamoto, Japan) (42). The second TFPIα ELISA was Asserachrom Free TFPI (Stago) in which a monoclonal antibody (2C6) was used as catcher and second monoclonal antibody against the C terminus (HG5) as detector.

Statistics. To analyze results of the QRT-PCR, the 1-tailed Student's *t* test was used. $P < 0.05$ was considered statistically significant.

Study approval. All participants gave written informed consent. The Institutional Review Board and the Center for Protection of Human Subjects at UTHSC-H approved this study (MS-02-157).

Acknowledgments

During performance of the initial part of this work, L.M. Vincent was a Schissler Foundation Fellow and D.M. Milewicz was a Doris Duke Distinguished Clinical Scientist. We would like to thank William P. Dubinsky at University of Texas Health Science Center at Houston Proteomics Core Laboratory for valuable discussions, Dongchuan Guo and Hariyadarshi Pannu, Van Tran-Fadulu, and the nurses of the CRC for their help in collecting patient samples. This work was supported by grants of the Doris Duke Foundation, NIH (UL1 RR024148; CTSA), the Swedish Research Council (#07143), the Heart-Lung Foundation, and the Söderberg's Foundation (to B. Dahlbäck). T. Hamuro at The Chemo-Sero-Therapeutic Research Institute is acknowledged for providing recombinant full-length TFPIα.

Received for publication January 29, 2013, and accepted in revised form May 30, 2013.

Address correspondence to: Dianna M. Milewicz, University of Texas Health Science Center at Houston, 6431 Fannin, MSB 6.100, Houston, Texas 77030, USA. Phone: 713.500.6715; Fax: 713.500.0693; E-mail: Dianna.M.Milewicz@uth.tmc.edu. Or to: Björn Dahlbäck, Lund University, Department of Laboratory Medicine, Wallenberg Laboratory, Inga Marie Nilsson's street 53, University Hospital, S-20502 Malmö, Sweden. Phone: 46.40.331501; Fax: 46.40.337044; E-mail: bjorn.dahlback@med.lu.se.

Lisa M. Vincent's present address is: Sr. Scientist II, GeneDx, Gaithersburg, Maryland, USA.

1. Nicolaes GA, Dahlbäck B. Factor V and thrombotic disease: description of a janus-faced protein. *Arterioscler Thromb Vasc Biol*. 2002;22(4):530–538.
2. Segers K, Dahlbäck B, Nicolaes GA. Coagulation factor V and thrombophilia: background and mechanisms. *Thromb Haemost*. 2007;98(3):530–542.
3. Cripe LD, Moore KD, Kane WH. Structure of the gene for human coagulation factor V. *Biochemistry*. 1992;31(15):3777–3785.
4. Jenny RJ, et al. Complete cDNA and derived amino acid sequence of human factor V. *Proc Natl Acad Sci U S A*. 1987;84(14):4846–4850.
5. Kane WH, Davie EW. Blood coagulation factors V and VIII: structural and functional similarities and their relationship to hemorrhagic and thrombotic disorders. *Blood*. 1988;71(3):539–555.
6. Kane WH, Ichinose A, Hagen FS, Davie EW. Cloning of cDNAs coding for the heavy chain region and connecting region of human factor V, a blood coagulation factor with four types of internal repeats. *Biochemistry*. 1987;26(20):6508–6514.
7. Wang H, Riddell DC, Guinto ER, MacGillivray RT, Hamerton JL. Localization of the gene encoding human factor V to chromosome 1q21-25. *Genomics*. 1988;2(4):324–328.
8. Mann KG, Nesheim ME, Tracy PB. Molecular weight of undegraded plasma factor V. *Biochemistry*. 1981;20(1):28–33.
9. Kane WH, Majerus PW. Purification and characterization of human coagulation factor V. *J Biol Chem*. 1981;256(2):1002–1007.
10. Nesheim ME, Foster WB, Hewick R, Mann KG. Characterization of Factor V activation intermediates. *J Biol Chem*. 1984;259(5):3187–3196.
11. Suzuki K, Dahlbäck B, Stenflo J. Thrombin-catalyzed activation of human coagulation factor V. *J Biol Chem*. 1982;257(11):6556–6564.
12. Tracy PB, Eide LL, Bowie EJ, Mann KG. Radioimmunoassay of factor V in human plasma and platelets. *Blood*. 1982;60(1):59–63.
13. Gould WR, Simioni P, Silveira JR, Tormene D, Kalafatis M, Tracy PB. Megakaryocytes endocytose and subsequently modify human factor V in vivo to form the entire pool of a unique platelet-derived cofactor. *J Thromb Haemost*. 2005;3(3):450–456.
14. Hayward CP, et al. Factor V is complexed with multimerin in resting platelet lysates and colocalizes with multimerin in platelet alpha-granules. *J Biol Chem*. 1995;270(10):19217–19224.
15. Hayward CP, Warkentin TE, Horsewood P, Kelton JG. Multimerin: a series of large disulfide-linked multimeric proteins within platelets. *Blood*. 1991;77(12):2556–2560.
16. Brummel KE, Paradis SG, Butenas S, Mann KG. Thrombin functions during tissue factor-induced blood coagulation. *Blood*. 2002;100(1):148–152.
17. Butenas S, Brummel KE, Branda RF, Paradis SG, Mann KG. Mechanism of factor VIIa-dependent coagulation in hemophilia blood. *Blood*. 2002;99(3):923–930.
18. Butenas S, van 't Veer C, Mann KG. Evaluation of the initiation phase of blood coagulation using ultrasensitive assays for serine proteases. *J Biol Chem*. 1997;272(34):21527–21533.
19. Hockin MF, Jones KC, Everse SJ, Mann KG. A model for the stoichiometric regulation of blood coagulation. *J Biol Chem*. 2002;277(21):18322–18333.
20. Nesheim ME, Myrmel KH, Hibbard L, Mann KG. Isolation and characterization of single chain bovine factor V. *J Biol Chem*. 1979;254(2):508–517.
21. Dahlbäck B. Advances in understanding pathogenic mechanisms of thrombophilic disorders. *Blood*. 2008;112(1):19–27.
22. Hockin MF, Kalafatis M, Shatos M, Mann KG. Protein C activation and factor Va inactivation on human umbilical vein endothelial cells. *Arterioscler Thromb Vasc Biol*. 1997;17(11):2765–2775.
23. Kalafatis M, Rand MD, Mann KG. The mechanism of inactivation of human factor V and human factor Va by activated protein C. *J Biol Chem*. 1994;269(50):31869–31880.
24. Duckers C, et al. Low plasma levels of tissue factor pathway inhibitor in patients with congenital factor V deficiency. *Blood*. 2008;112(9):3615–3623.
25. Broze GJ Jr, Girard TJ. Tissue factor pathway inhibitor: structure-function. *Front Biosci*. 2012;17:262–280.
26. Girard TJ, Tuley E, Broze GJ Jr. TFPIβ is the GPI-anchored TFPI isoform on human endothelial cells and placental microsomes. *Blood*. 2012;119(5):1256–1262.
27. Ndonwi M, Girard TJ, Broze GJ Jr. The C-terminus of tissue factor pathway inhibitor α is required for its interaction with factors V and Va. *J Thromb Haemost*. 2012;10(9):1944–1946.
28. Kuang SQ, et al. Characterization of a novel autosomal dominant bleeding disorder in a large kindred from east Texas. *Blood*. 2001;97(6):1549–1554.
29. Blanchette M, et al. Aligning multiple genomic sequences with the threaded blockset aligner. *Genome Res*. 2004;14(4):708–715.
30. Camire RM, Bos MH. The molecular basis of fac-

tor V and VIII procofactor activation. *J Thromb Haemost*. 2009;7(12):1951–1961.
31. Norstrøm E, Thorelli E, Dahlbäck B. Functional characterization of recombinant FV Hong Kong and FV Cambridge. *Blood*. 2002;100(2):524–530.
32. Bos MH, Camire RM. A bipartite autoinhibitory region within the B-domain suppresses function in factor V. *J Biol Chem*. 2012;287(31):26342–26351.
33. Petersen LC. Hemostatic properties of a TFPI antibody. *Thromb Res*. 2012;129(suppl 2):S44–S45.
34. Swart AC, Klaassen BH, Bloys-van Treslong-de, Hemker HC. The adsorption of blood coagulation factors II, VII, IX and X from human plasma to aluminium hydroxide. *Thromb Diath Haemorrh*. 1972;27(3):490–501.
35. Dahlbäck B, Hildebrand B. Inherited resistance to activated protein C is corrected by anticoagulant cofactor activity found to be a property of factor V. *Proc Natl Acad Sci U S A*. 1994;91(4):1396–1400.
36. Kaufman RJ. Vectors used for expression in mammalian cells. *Methods Enzymol*. 1990;185:487–511.
37. Pittman DD, Tomkinson KN, Kaufman RJ. Post-translational requirements for functional factor V and factor VIII secretion in mammalian cells. *J Biol Chem*. 1994;269(25):17329–17337.
38. Pittman DD, Tomkinson KN, Michnick D, Selighsohn U, Kaufman RJ. Posttranslational sulfation of factor V is required for efficient thrombin cleavage and activation and for full procoagulant activity. *Biochemistry*. 1994;33(22):6952–6959.
39. Hackeng TM, Seré KM, Tans G, Rosing J. Protein S stimulates inhibition of the tissue factor pathway by tissue factor pathway inhibitor. *Proc Natl Acad Sci U S A*. 2006;103(9):3106–3111.
40. Sun YH, Tran S, Norstrøm EA, Dahlbäck B. Enhanced rate of cleavage at Arg-306 and Arg-506 in coagulation factor Va by Gla domain-mutated human-activated protein C. *J Biol Chem*. 2004;279(46):47528–47535.
41. Tran S, Norstrøm E, Dahlbäck B. Effects of prothrombin on the individual activated protein C-mediated cleavages of coagulation factor Va. *J Biol Chem*. 2008;283(11):6648–6655.
42. Nakahara Y, et al. Amino acid sequence and carbohydrate structure of a recombinant human tissue factor pathway inhibitor expressed in Chinese hamster ovary cells: one N- and two O-linked carbohydrate chains are located between Kunitz domains 2 and 3 and one N-linked carbohydrate chain is in Kunitz domain 2. *Biochemistry*. 1996;35(20):6450–6459.